Energy Proceedings
Vol 50, 2025
ISSN 2004-2965

Part-load performance analysis of an intercooled and recuperative gas turbine system integrated with transcritical organic Rankine cycle#

Yanbing Dai[1], Xiaoqu Han[1*], Xuanhua Guo[2], Junjie Yan[1]

1 State Key Laboratory of Multiphase Flow in Power Engineering, Xi'an Jiaotong University, Xi'an 710049, China

2 Qingdao Huaru Energy Technology Company Limited, Qingdao 266071, China
(*Xiaoqu Han: hanxiaoqu@mail.xjtu.edu.cn)

ABSTRACT

Gas turbine propulsion systems are widely used in modern commercial ships due to their high power density, reliability, and operational flexibility. However, their efficiency often drops significantly under varying load conditions. To address this issue, a novel intercooled and recuperative gas turbine system integrated with transcritical organic Rankine cycle (ICR-GT-TORC) was proposed in the present work. The system performance was evaluated under both design and off-design conditions using thermodynamic and off-design models developed with Thermoflex software. Comparative analysis with conventional UGT25000 marine gas turbines revealed that the ICR-GT-TORC system achieved an efficiency of 49.4% and a power output of 38.1 MW, reflecting improvements of 29.3% and 37.6%, respectively. Moreover, the ICR-GT-TORC and ICR-GT system demonstrated significant advantages under part-load conditions. At 30% load, the efficiency of the ICR-GT-TORC system remained high at 43.7%, with a reduction of 11.5%. The ICR-GT system maintained an efficiency of 40.9%, with only a 7.9% reduction. In contrast, the efficiency of the simple cycle dropped significantly to 28.4%, with a 25.7% decrease. These findings could provide valuable insights into optimizing marine propulsion systems for off-design performance.

Keywords: gas turbine, transcritical organic Rankine cycle, intercooler, recuperator, off-design performance

NONMENCLATURE

Abbreviations	
LHV	lower heating value
OWF	organic working fluid
Symbols	
P	power
ε	heat exchanger effectiveness
ξ	cooling air fraction
ϕ	relative humidity

1. INTRODUCTION

The maritime industry significantly contributes to global greenhouse gas (GHG) emissions, making the enhancement of marine gas turbine efficiency a priority. The International Maritime Organization has set ambitious targets to reduce GHG emissions from ships by at least 40% by 2030, compared to 2008 level [1]. Marine gas turbines, widely used for their reliability and high power density, often experience considerable efficiency losses under part-load conditions. These inefficiencies pose a challenge in meeting environmental regulations and maintaining the economic viability of maritime operations. The global marine gas turbine market, valued at hundreds of millions of dollars, is projected to grow steadily, driven by the increasing demand for efficient and reliable propulsion in both civil and military sectors [2]. As the market expands, optimizing the off-design performance of marine gas turbines becomes increasingly critical to ensuring compliance with stringent emissions targets and the sustainable operation of shipping fleets in a highly regulated industry.

Significant progress has been made in the research on marine gas turbines, especially in developing configuration improvements aimed at enhancing efficiency and reducing emissions. One major focus has been the adoption of advanced cycles, such as intercooling and recuperation heat recovery. Intercooling has been explored for its ability to reduce compression work by cooling the air between low-pressure compressor (LPC) and high-pressure compressor (HPC) [3-4]. Recuperative cycles, on the other hand, utilize waste heat from the turbine exhaust gas to preheat the compressed air before combustion,

This is a paper for the 16th International Conference on Applied Energy (ICAE2024), Sep. 1-5, 2024, Niigata, Japan.

thereby improving overall cycle efficiency [5]. This approach is particularly advantageous in marine applications, where space and weight are critical factors. In addition to these configurations, the integration of bottoming cycles, such as the Organic Rankine Cycle (ORC), has been studied. These coupled cycles leverage waste heat recovery to further enhance the energy output and efficiency of gas turbines, with the supercritical CO_2-ORC combined cycle showing particularly promising results in reducing emissions and improving energy efficiency [6]. In parallel, research on off-design performance has focused on understanding and predicting the behavior of gas turbines under varying operational conditions. This has led to the development of advanced performance prediction tools [7-8], such as compressor performance maps, which account for variables like ambient temperature and pressure. These tools are essential for accurately predicting how gas turbines will perform under different load conditions, a critical aspect given the fluctuating operational environments encountered in marine applications [9]. Furthermore, control strategies have been a key area of study, with researchers developing methods like gain-scheduling and real-time optimization of variable stator vanes to enhance the adaptability of gas turbines to changing operational demands [10]. These strategies are crucial for maintaining efficiency and operational stability, especially in the dynamic and often harsh conditions at sea [11].

Despite these advancements, there remains a lack of comprehensive studies that fully integrate configuration optimization with off-design performance analysis. Therefore, a novel intercooled and recuperative gas turbine system integrated with transcritical Organic Rankine Cycle (ICR-GT-TORC) was proposed in the present work. Thermodynamic analysis of the system under design conditions was conducted based on simulation modeling. Additionally, the system performance was analyzed under off-design conditions, with a particular focus on part-load scenarios.

2. DESIGN OF THE ICR-GT-TORC SYSTEM

2.1 System configuration

A UGT25000 marine gas turbine simple cycle is taken as the case unit, as illustrated in Fig. 1. This unit features a three-shaft design, consisting of a two-spool gas generator and a free power turbine. The two-spool gas generator includes two axial flow compressors (a 9-stage LPC and a 9-stage HPC) each driven by its own turbine (a 1-stage low-pressure turbine (LPT) and a 1-stage high-pressure turbine (HPT)), and a loop-shaped cannular combustor. The power turbine operates independently of the gas generator and can be configured in either reversible or non-reversible versions, with varying speeds and rotation directions.

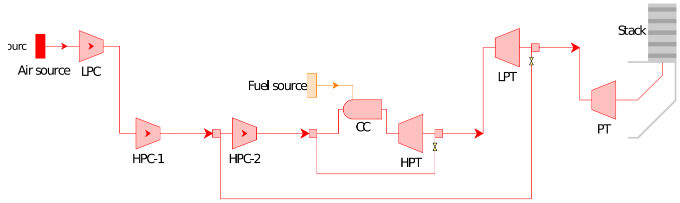

Fig. 1. UGT25000 simple cycle

An intercooler is installed between the LPC and the HPC to cool the air entering the HPC. This setup reduces the inlet temperature of the HPC, thereby decreasing the work required by the HPC and significantly enhancing system power output. Additionally, a recuperator is added to recover waste heat from the turbine exhaust, which is then used to preheat the air entering the combustion chamber. This configuration, known as the intercooled and recuperative gas turbine (ICR-GT), as shown in Fig. 2, is similar to the system design used in the WR-21 marine gas turbine [12].

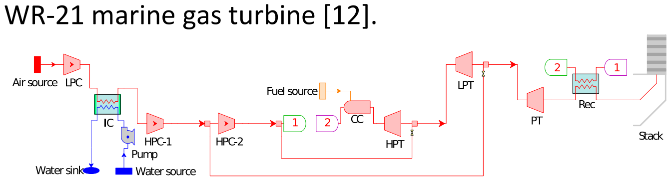

Fig. 2. ICR-GT system

By further integrating a TORC to recover waste heat from exhaust gases, an ICR-GT-TORC system is formed, as depicted in Fig. 3. In previous work by the authors, a dual-stage intercooled and recuperative gas turbine system integrated with a transcritical organic Rankine cycle was proposed for land-based power generation, with its performance evaluated under design conditions [5]. The ICR-GT-TORC system proposed in the present work is primarily designed for marine propulsion applications, with a focus on its performance under part-load conditions.

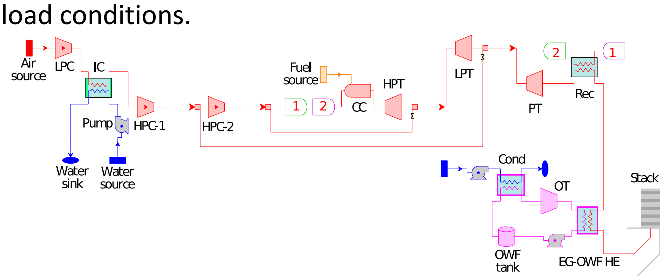

Fig. 3. ICR-GT-TORC system

2.2 Operation strategy

For the UGT25000 simple cycle, a constant turbine exhaust temperature (*TET*) operation mode is used at high loads (64%–100%), with regulation achieved through a combination of inlet guide vane (IGV) control and fuel flow control. In the ICR-GT and ICR-GT-TORC systems, a constant turbine inlet temperature (*TIT*) mode is employed at high loads (87%–100%), where IGV and fuel flow controls adjust power output. In the medium load range (75%–87%), the low-pressure shaft operates at maximum speed, with power adjusted via IGV and fuel flow control. At low loads, all three systems use fuel flow control exclusively. Detailed control methods for the three systems are shown in Table 1.

Table 1. Operation strategies of different configurations

Configuration	Load range	Operation mode	Control method
Simple cycle	64%-100%	Constant TET operation	IGV + Fuel flow
	Below 64%	/	Fuel flow
ICR-GT system	87%-100%	Constant *TIT*	IGV + Fuel flow
	75%-87%	Constant N_{LP}	IGV + Fuel flow
	Below 75%	/	Fuel flow
ICR-GT-TORC system	87%-100%	Constant *TIT*	IGV + Fuel flow
	75%-87%	Constant N_{LP}	IGV + Fuel flow
	Below 75%	/	Fuel flow

3. MODELS AND METHODOLOGY

A model combining thermodynamic design with off-design performance analysis was established to evaluate the performance of marine gas turbines across the entire load range. The cooling air modeling was simplified [13], assuming that the cooling air mixed directly with the main flow exiting the cooled turbines. High-pressure cooling air, extracted from the HPC outlet, was used to cool the HPT, while air extracted after the fifth stage of the HPC was used for cooling the LPT [14].

3.1 Thermodynamic models

The energy equations for different configurations and their components can refer to the authors' previous work [5].

Due to the lack of real operational data, the efficiency of the UGT25000 compressors at design conditions is estimated using the following formula [15]:

$$\eta_C = \frac{\pi_C^m - 1}{\pi_C^{\frac{m}{\eta_{s,C}}} - 1} \tag{1}$$

where π_c is the pressure ratio of the compressor; $m=\frac{k-1}{k}$; k is the specific heat ratio (1.40 for estimating the compressor efficiency at design conditions); and $\eta_{s,C}$ is the efficiency of the single compressor stage (0.91 for LPC, and 0.89 for HPC).

The pressure coefficient (v) is generally defined as the following:

$$v = \frac{p_{out}}{p_{in}} \tag{2}$$

3.2 Off-design models

3.2.1 Compressor

The off-design performance of compressors is calculated using the dimensionless compressor map for fully open IGVs built into the Thermoflex software, as presented in Fig. 4.

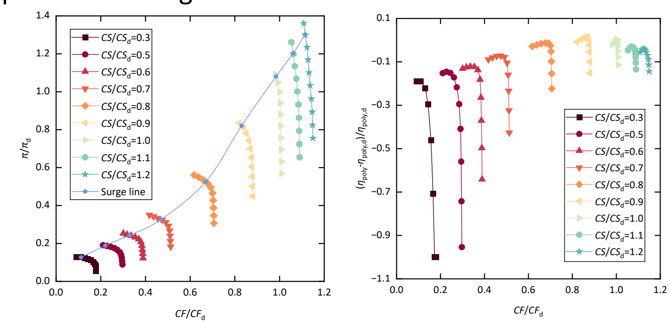

(a) Characteristic curves of pressure ratio (b) Characteristic curves of efficiency

Fig. 4. Dimensionless compressor map

The corrected flow (CF/kg·s^{-1}) is defined as:

$$CF = \frac{\dot{m}\sqrt{T_{in} / T_{ref}}}{M\left(p_{in} / p_{ref}\right)} \tag{3}$$

where $\dot{m}$ is the mass flow rate (kg·s^{-1}); T_{in} is the inlet temperature; T_{ref} is the reference temperature (288.15 K); M is the molecular weight; p_{in} is the inlet pressure (kPa); and p_{ref} is the reference pressure (101.325 kPa).

The corrected speed (CS/r·min^{-1}) is formulated as:

$$CS = N\sqrt{p_{in} / p_{ref}} \tag{4}$$

where N is the actual rotational speed (r·min^{-1}).

When the IGVs are partially open, the reduced corrected flow is calculated using the following equation:

$$CF_{PO} = CF_{FO} \cdot \left[1 - \left(1 - X_{10}\right) \cdot \left(1 - X_{11}\right)\right] \tag{5}$$

where CF_{PO} is the corrected flow for IGVs partially open (kg·s^{-1}); CF_{FO} is the corrected flow for IGVs fully open (kg·s^{-1}); X_{10} is the ratio of the mass flow rate for IGVs fully closed to the mass flow rate for IGVs fully open (0.75);

and X_{11} is the ratio of the current IGVs opening (1 for fully opening, and 0 for fully closed).

3.2.2 Turbine

The off-design performance of turbines is calculated using the dimensionless turbine map built into the Thermoflex software, as shown in Fig. 5.

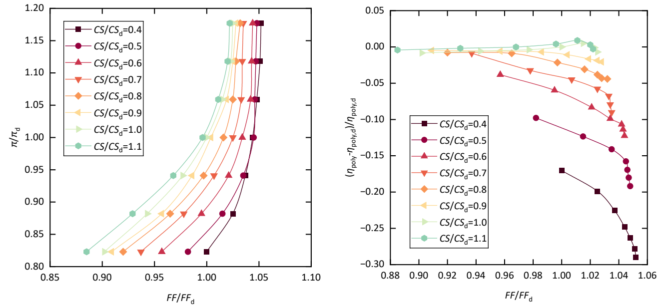

(a) Characteristic curves of pressure ratio

(b) Characteristic curves of efficiency

Fig. 5. Dimensionless turbine map

The flow function (FF/m^2) is defined as:

$$FF = \frac{C\dot{m}}{p_{in}}\sqrt{\frac{\left(\frac{R}{M\cdot k}\right)T_{in}}{\left(\frac{2}{k+1}\right)^{\frac{k+1}{k-1}}}} \tag{6}$$

where C is the dimensional constant (31.62 m^2·Pa·[(kg·s^{-1})·(J·kg^{-1})$^{0.5}$]$^{-1}$); and R is the gas constant (8.314 J·(mol·K)$^{-1}$).

4. RESULTS AND DESCUSSION

4.1 System design and thermodynamic analysis

The fundamental assumptions for the system design and performance analysis are detailed in Table 2. Additionally, the thermodynamic model for the UGT25000 simple cycle gas turbine was validated by comparing it with existing reference data [16], as shown in Table 3. The results indicated that the performance parameters closely matched the reference values when using the same input parameters.

Table 2. Design parameters and main assumptions of different configurations at design conditions

Parameter	Value			Reference
	Simple cycle	ICR-GT system	ICR-GT-TORC system	
Fuel	Distillate oil	Distillate oil	Distillate oil	[16]
LHV/kJ·kg^{-1}	42330	42330	42330	[16-17]
T_0/°C	15	15	15	[18]
p_0/kPa	101.325	101.325	101.325	[18]
ϕ_0/%	60	60	60	[18]
$\dot{m}_{air}$/kg·s^{-1}	92.19	92.19	92.19	[16]
TIT/°C	1250	1250	1250	[19]
π_C	22.5	22.5	22.5	[16]
π_{LPC}	4.743	4.743	4.743	
π_{HPC}	4.743	4.743	4.743	
η_{LPC}/%	88.87	88.87	88.87	
η_{HPC}/%	86.40	86.40	86.40	
η_{LPT}/%	89.00	89.00	89.00	[15]
η_{HPT}/%	87.50	87.50	87.50	[15]
η_{PT}/%	91.00	91.00	91.00	[15]
N_{LP}/r·min^{-1}	6200	6200	6200	[20]
N_{HP}/r·min^{-1}	8100	8100	8100	[20]
N_{PT}/r·min^{-1}	3460	3460	3460	[16]
v_{CC}	0.96	0.96	0.96	[15]
ξ_{LPT}/%	3.61	3.61	3.61	[14]
ξ_{HPT}/%	15.12	15.12	15.12	[14]
$T_{IC,gas,out}$/°C	/	60	60	[5]
ε_{Rec}/%	/	88.5	88.5	
η_{Pump}/%	/	75	75	
OWF	/	/	R1336mzz(Z)	
$p_{OT,in}$/MPa	/	/	3.1	
$T_{OT,in}$/°C	/	/	179	
p_{cond}/kPa	/	/	102	[5]

Table 3. Validation of the UGT25000 simple cycle model

Performance parameter	Reference [16]	Present work	Relative deviation/%
ISO base load/kW	28709	28402	-1.07
SFC/g·kWh^{-1}	227.5	222.6	-2.15
Heat rate/kJ·kWh^{-1}	9732	9423	-3.34
η_{sys}/%	37.00	38.20	3.25
$\dot{m}_{EG}$/kg·s^{-1}	94.00	93.94	-0.06
T_{EG}/°C	500	468	-6.35

Based on the above assumptions, thermodynamic design was conducted for different configurations, and the main performance results are presented in Table 4. Compared to the simple cycle, the ICR-GT and ICR-GT-TORC systems increased power output by 23.9% and 37.6%, respectively, while reducing specific fuel consumption (*SFC*) by 13.9% and 22.6%. The system efficiency improved by 16.2% and 29.3%, respectively. The results demonstrated that integrating intercooling, recuperation, and further coupling with a transcritical organic Rankine cycle (TORC) can significantly improve system performance at design conditions.

Table 4. Performance comparison of different configurations at design conditions

Performance parameter	Simple cycle	ICR-GT	ICR-GT-TORC
Power output/kW	28402	35192	39073
SFC/g·kWh^{-1}	222.6	191.6	172.2
Heat rate/kJ·kWh^{-1}	9423	8109	7290
η_{sys}/%	38.20	44.40	49.38
$\dot{m}_{EG}$/kg·s^{-1}	93.94	94.06	94.06
T_{EG}/°C	468	325	90

4.2 Part-load performance of different configurations

The part-load performance of system efficiency and power output for different configurations are illustrated in Fig. 6. Compared to the simple cycle and ICR-GT system, the ICR-GT-TORC system consistently achieved higher efficiency and power output across the 30% to 100% load range. At 30% load, the efficiency of the ICR-GT-TORC system is 53.8% and 6.8% higher, and its power output is 44.3% and 8.9% higher than those of the simple cycle and ICR-GT system, respectively. However, the ICR-GT system demonstrated the strongest load adaptability among the three configurations. As the load decreased from 100% to 30%, the system efficiency dropped by 25.7%, 7.9%, and 11.5% for the simple cycle, the ICR-GT system, and the ICR-GT-TORC system, respectively.

The range from the terminal exhaust gas temperature (T_{EG}) to the *TIT* intuitively reflected the temperature utilization range of the three systems, as depicted in Fig. 7. The ICR-GT and ICR-GT-TORC systems, which used the same load control strategy, showed consistent trends in *TIT* variation with load. Their *TIT* was generally higher than that of the simple cycle across most load ranges. The ICR-GT-TORC system maximized exhaust gas waste heat recovery via the recuperator and TORC bottoming cycle, maintaining a T_{EG} between 88 °C and 97 °C across different loads. The ICR-GT system, which used a recuperator to recover part of the exhaust gas waste heat, showed a T_{EG} range of 253 °C to 326 °C for loads between 30% and 100%. In contrast, the simple cycle, which did not recover exhaust gas waste heat, had a T_{EG} range of 428 °C to 469 °C. Therefore, the temperature utilization range across different loads, from widest to narrowest, followed the order of ICR-GT-TORC, ICR-GT, and the simple cycle, corresponding to their efficiency ranking.

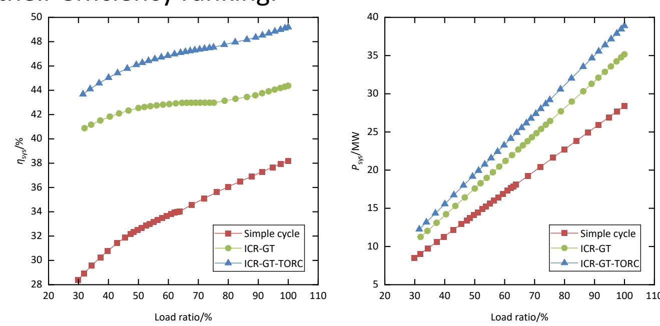

(a) η_{sys} (b) P_{sys}

Fig. 6. Variation in system efficiency and power output with load ratio for different configurations

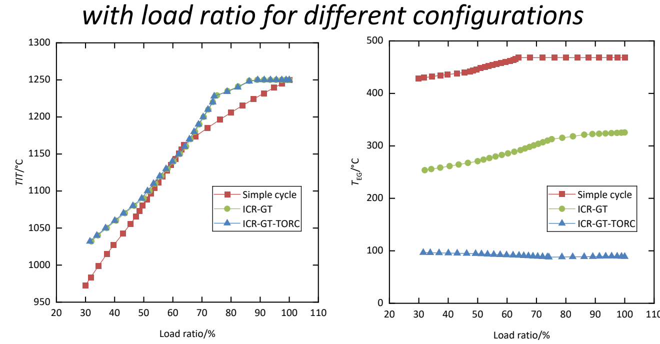

(a) *TIT* (b) T_{EG}

Fig. 7. Variation in turbine inlet temperature and terminal exhaust gas temperature with load ratio for different configurations

5. CONCLUSIONS

Traditional marine gas turbines experience significant efficiency drops under part-load conditions, making configuration optimization a critical solution. In the present work, the UGT25000 simple cycle was modified into the ICR-GT and ICR-GT-TORC systems, and their performance was analyzed under both design and off-design conditions. The results demonstrated that the

ICR-GT-TORC system enabled highly efficient operation across the entire load range, with system efficiency increasing by up to 29.3% and power output by up to 37.6% under design conditions, compared to the traditional simple cycle and ICR-GT system. At low loads, the ICR-GT-TORC system achieved the highest efficiency, maintaining 43.7% efficiency at 30% load, while the ICR-GT system exhibited the strongest load adaptability with only a 7.9% efficiency decrease as the load decreased from 100% to 30%. The energy-saving mechanism of the ICR-GT-TORC system was driven by effective exhaust gas waste heat recovery, which broadened the temperature utilization range. Through the use of a recuperator and the TORC bottoming cycle to recover heat energy from the exhaust gases, the system maintained a terminal exhaust temperature between 88°C and 97°C during part-load operation.

ACKNOWLEDGEMENT

This work was supported by the Energy Security Technology Research Project of Huaneng Group Science and Technology Foundation (No. HNKJ20-H87) and the Innovative Scientific Program of CNNC.

REFERENCE

[1] International Maritime Organization. (2023). *2023 IMO Strategy on Reduction of GHG Emissions from Ships*.https://www.imo.org/en/OurWork/Environment/Pages/2023-IMO-Strategy-on-Reduction-of-GHG-Emissions-from-Ships.aspx

[2] Mordor Intelligence. *Naval Gas Turbine Market Size & Share Analysis - Growth Trends & Forecasts (2024 - 2029)*. https://www.mordorintelligence.com/industry-reports/naval-gas-turbine-market

[3] Cheng, X., Zheng, H., Dong, W., & Yang, X. (2023). Performance prediction of marine intercooled cycle gas turbine based on expanded similarity parameters. *Energy*, *265*, 126402.

[4] Ji, N., Li, S., Wang, Z., & Zhao, N. (2017). Off-design behavior analysis and operating curve design of marine intercooled gas turbine. *Math Probl Eng*, *2017*, 8325040.

[5] Han, X., Dai, Y., Guo, X., Braimakis, K., Karellas, S., & Yan, J. (2024). A novel dual-stage intercooled and recuperative gas turbine system integrated with transcritical organic Rankine cycle: System modeling, energy and exergy analyses. *Energy*, *305*, 132252.

[6] Hou, S., Zhang, F., & Yang, Q. (2024). Comparative analysis of supercritical CO_2-ORC combined cycle for gas turbine waste heat recovery based on multi-objective optimization. *Appl Therm Eng*, *236*, 121776.

[7] Hao, X., Sun, L., Chi, J., & Zhang, S. (2022). Off-design performance of 9F gas turbine based on gPROMs and BP neural network model. *J Therm Sci*, *31*(1), 261-272.

[8] Li, Y. G., Ghafir, M. F. A., Wang, L., Singh, R., Huang, K., & Feng, X. (2011). Nonlinear multiple points gas turbine off-design performance adaptation using a genetic algorithm. *J Eng Gas Turb Power*, *133*(7), 071701.

[9] Machmudah, A., Lemma, T. A., Solihin, M. I., Feriadi, Y., Rajabi, A., Afandi, M. I., & Abbasi, A. (2022). Design optimization of a gas turbine engine for marine applications: Off-design performance and control system considerations. *Entropy*, *24*(12), 1729.

[10] Wang, Z., Li, J., Fan, K., & Li, S. (2017). The off-design performance simulation of marine gas turbine based on optimum scheduling of variable stator vanes. *Math Probl Eng*, *2017*, 2671251.

[11] Hosseinimaab, S. M., & Tousi, A. M. (2021). A new approach to off-design performance analysis of gas turbine engines and its application. *Energy Convers Manage*, *243*, 114411.

[12] Weller, C. L., Broadbelt, A., & Law, B. (1996). WR-21 Design and Maintenance. *Proceedings of the ASME 1996 International Gas Turbine and Aeroengine Congress and Exhibition*, *UK*, *2*, 96-GT-328.

[13] Gülen, S. C. (2019). *Gas turbines for electric power generation*. Cambridge University Press.

[14] Wang, W., Chen, L., & Sun, F. (2011). Thermodynamic modeling and performance optimization for simple-cycle gas turbine with air cooling: (I) Modeling. *Therm Turb*, *40*(4), 245-249.

[15] Liu, K., Chen, D., Serbin, S., & Patlaichuk, V. (2023). *Gas Turbines Structural Properties, Operation Principles and Design Features*. Springer Singapore.

[16] Gas Turbine World. (2023). *2023 GTW Handbook*. Pequot Publishing Inc.

[17] Thermoflow. *THERMOFLEX® - General Purpose Program for design & simulation of gas turbine combined cycles, cogeneration systems, conventional steam plants, renewable energy and other thermal systems*. https://www.thermoflow.com/products_generalpurpose.html

[18] International Organization for Standardization. (2016). *Gas turbine applications - Requirements for power generation* (ISO Standard No. 19859:2016).

[19] Wen, X., Ren, L., Qi, L., & Hong, Q. (2020). Development and key technologies in marine gas turbine. *J Propul Tech*, *41*(11), 2401-2407.

[20] Rolls-Royce WR-21. (2024, March 5). In *Wikipedia*. https://en.wikipedia.org/wiki/Rolls-Royce_WR-21